

Optimization of a Dual-Energy Contrast-Enhanced Technique for a Photon Counting Digital Breast Tomosynthesis System

Ann-Katherine Carton¹, Christer Ullberg², Karin Lindman², Tom Francke²,
and Andrew Maidment¹

¹ University of Pennsylvania, Dept. Radiology, 3400 Spruce St., 19104 Philadelphia PA

² XCounter AB, Svärdvägen 11, SE-182 33 Danderyd, Sweden

{Ann-Katherine.Carton, Andrew.Maidment}@uphs.upenn,
{Christer.Ullberg, Karin.Lindman, Tom.Francke}@XCounter.se

Abstract. We have developed a dual-energy technique for contrast-enhanced digital breast tomosynthesis using a photon-counting imaging system whereby low- and high-energy images are acquired in a single scan. A W target x-ray source is employed at 49 kV. Sn and Cu filters are used to obtain low- and high-energy images. Iodine enhanced images are calculated by applying a weighted subtraction to the logarithm of the Sn and Cu images. The optimal system configuration and Sn-Cu filter pair were assessed using theoretical modeling. The mean glandular dose was kept to 1 mSv. Optimal weighting factors (w_i) for the subtraction and *SDNR* between iodine-enhanced and non-enhanced breast background were calculated. Optimal w_i and *SDNR* depend on the Sn-Cu combination and breast thickness. *SDNR* varies with the dose allocated among the Sn and Cu images. The optimal configuration uses Sn and Cu filters of sufficient thickness to require the maximum mAs achievable by the x-ray tube.

Keywords: Contrast-Enhanced Digital Breast Tomosynthesis, Dual Energy Subtraction, Temporal Subtraction, vascular contrast agent.

1 Introduction

Today, MRI using gadolinium chelates as a vascular contrast agent is the standard to image the vasculature of breast cancers [1]. Preliminary studies have demonstrated that contrast-enhanced digital breast tomosynthesis (CE-DBT) using an iodinated vascular contrast agent has the potential to rival CE-MRI [2].

Two CE-DBT techniques have been proposed: temporal and dual-energy (DE) subtraction. In temporal subtraction, one pre- and one or more post-contrast DBT image series are acquired using a spectrum that extends above the K-edge of iodine (33.2 keV). The pre- and post-contrast image series are then logarithmically subtracted yielding iodine enhanced images. DE CE-DBT only requires that post-contrast image series be acquired at two energies that closely bracket the K-absorption edge of iodine. At each time point, iodine-enhanced images are calculated by weighted logarithmic subtraction of the low- and high-energy (LE and HE) images.

Any breast motion between DBT series, however, will result in registration artifacts in the subtraction images resulting in an erroneous estimate of the iodine uptake. Temporal subtraction CE-DBT is prone to significant motion artifacts due to the extended time delay (up to 10 minutes) between the pre- and post-contrast series [3]. DE CE-DBT is much less sensitive to breast motion because the LE and HE images can be acquired simultaneously or in rapid succession for any time point.

This paper details a DE CE-DBT technique developed on a photon-counting DBT imaging system. In our system configuration, the LE and HE images are acquired in a single scan. Simultaneous image acquisition minimizes the risk of patient motion but requires the LE and HE images to be acquired with the same target material, kV and mA. We have conducted theoretical modeling to optimize the system design and determine the optimal feasible acquisition parameters.

2 Material and Methods

2.1 Imaging System

The optimization for DE CE-DBT was performed for a photon-counting DBT system (XC Mammo-3T, XCounter AB, Danderyd, Sweden) described in detail previously [4, 5]. The design of the system is shown in Fig. 1. The imaging system consists of 48 photon-counting linear detectors which are precisely aligned with the focal spot of the x-ray source. A pre-collimator is positioned above the breast and defines 48 fan-shaped beams, each aligned with a detector and the focal spot. The x-ray source, pre-collimator and the digital detectors are mounted on an E-arm and translated across the breast in a continuous linear motion; each linear detector collects an image at a distinct angle. The system geometry results in almost scatter free images. The detector technology is quantum limited and does not contribute any electronic noise; it is also free of lag and has a large dynamic range.

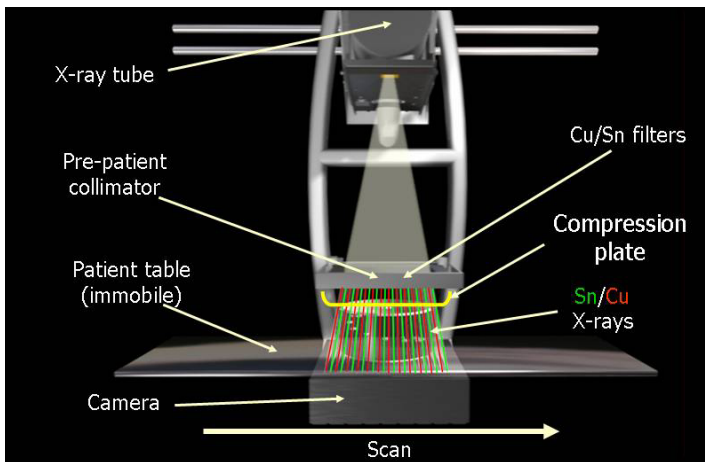


Fig. 1. DE implementation of the photon counting XC Mammo-3T

DE CE-DBT images are acquired using a W-target at 49 kV. Images with average energies that closely bracket the K-edge of iodine contrast agent (33.2 keV) are acquired in a single scan. We have investigated the use of Sn filters (0.08 to 0.22 mm) to produce images with average energy below the K-edge of iodine and Cu filters (0.11 to 0.27 mm) to produce images with average energy above the K-edge of iodine. The number of detectors allocated to the Sn and Cu images determines the signal-difference-to-noise-ratio (*SDNR*). With this in mind, we examined two system configurations. In the first configuration, the 48 fan beams are alternately filtered by Sn and Cu; as such, 24 of the detectors capture a Sn x-ray image and 24 capture a Cu x-ray image (This system configuration is hereafter referred to as 1:1). In the second configuration, 1 Sn filter is alternated with 2 Cu filters. In this way 16 Sn and 32 Cu projection images are obtained (This system configuration is hereafter referred to as 1:2). In both configurations, the scan time is 10 seconds.

2.2 Image Processing

Three dimensional tomographic images (referred to as DBT images) are reconstructed using a simple back-projection algorithm.

Iodine enhanced DE CE-DBT images are produced by applying a weighted subtraction to the logarithm of the Cu and Sn DBT images:

$$\overline{SI}_{DE}^{DBT} = \ln\left(\overline{SI}_{Cu}^{DBT}\right) - w_i \cdot \ln\left(\overline{SI}_{Sn}^{DBT}\right) \quad (1)$$

where \overline{SI}_{DE}^{DBT} , \overline{SI}_{Cu}^{DBT} and \overline{SI}_{Sn}^{DBT} denote the average signal intensity (*SI*) in a DE, Cu, and Sn DBT image. The weighting factor, w_i , acts as a tissue cancellation factor that can be optimized to maximize the *SDNR* between iodine contrast agent enhancement in a breast lesion and the background.

2.3 Theoretical Model

We have developed a computer model to simulate the DE implementation of the XC Mammo-3T photon counting acquisition system operated at 49 kV. The model is based upon the differential attenuation of x rays. The average detected *SI* per pixel in the Sn and Cu images, \overline{SI}_{Sn} and \overline{SI}_{Cu} was calculated as the absorbed primary x-ray photon fluence per pixel. The model ignored electronic noise and scatter; both are known to be small in the real system. DBT images were calculated with simple back-projection; thus \overline{SI}_{Sn}^{DBT} and \overline{SI}_{Cu}^{DBT} were simulated by summing \overline{SI}_{Sn} and \overline{SI}_{Cu} over the projection images that contribute to the respective DBT series. The standard deviations in \overline{SI}_{Sn}^{DBT} and \overline{SI}_{Cu}^{DBT} are proportional to the standard deviations of a Poisson distribution with an excess factor, $\epsilon_{DBT} = 1.18 \pm 0.03$. \overline{SI}_{DE}^{DBT} was calculated as in Eq. 1.

The standard deviation of the noise in \overline{SI}_{DE}^{DBT} was calculated as:

$$\sigma_{DE}^{DBT} = \epsilon_{DBT} \times \sqrt{\frac{1}{\overline{SI}_{Cu}^{DBT}} + w_i^2 \frac{1}{\overline{SI}_{Sn}^{DBT}}} \quad (2)$$

W-target spectra were calculated using a validated extrapolation of Boone's mammography spectra [3]. They were shaped using the Lambert-Beer law with appropriate mass attenuation coefficients and areal densities of the system parameters (inherent tube filtration, Sn and Cu filter thicknesses, air, compression plate, detector gas) and breasts (20 to 80 mm thick). The geometry of the breast was modeled as specified by Boone [6]; the breast consists of a mixture of glandular and adipose tissue surrounded by a 4 mm thick skin layer. Our computer model has been extensively validated experimentally [7].

2.4 Optimal Weighting Factor w_t

Weighting factors, w_t , for the logarithmic subtraction were calculated to optimally cancel the contrast between breast tissues with two different glandular fractions using the method described in [7]. The computations were repeated for all studied Sn-Cu filter pairs and for 20 to 80 mm thick breasts with extreme glandular tissue densities, f_g , between 0% and 50%.

2.5 Dose Allocation Optimization

To measure the detectability of iodine in DE CE-DBT images, we calculated the $SDNR$ between background breast tissue, B , and iodine enhanced breast tissue, I , normalized to the square root of the total mean glandular dose (MGD_{Total}). $SDNR$ was calculated per pixel as:

$$SDNR = \frac{\overline{SI}_{DE_B}^{DBT} - \overline{SI}_{DE_I}^{DBT}}{\sigma_{DE_B}^{DBT}}. \quad (3)$$

MGD_{Total} is calculated as $MGD_{Total} = MGD_{Sn} + MGD_{Cu}$, where MGD_{Sn} and MGD_{Cu} are the MGD allocated to the Sn and the Cu images. $SDNR/\sqrt{MGD_{Total}}$ was calculated as a function of the MGD fraction allocated to the Cu x-ray beam. Maximum $SDNR/\sqrt{MGD_{Total}}$, $SDNR_{max}/\sqrt{MGD_{Total}}$, and the resultant MGD fraction allocated to the Cu x-ray beam were calculated.

Breast entrance air kerma, K , of the spectra were required to calculate $SDNR$ corresponding to a given MGD . K were calculated using the method of Boone [6]:

$$K(S, L + t_{skin}, f_g) = \frac{MGD}{pDgN(S, L + t_{skin}, f_g)}, \quad (4)$$

where $pDgN$ is the MGD per unit breast entrance dose; $pDgN$ is a function of the spectrum (S), breast thickness ($L + t_{skin}$) and breast density f_g .

The mA values to obtain $SDNR_{max}/\sqrt{MGD_{Total}}$ were calculated. The calculations were performed for the 1:1 and the 1:2 system configurations, assuming $MGD_{Total} = 1\text{mSv}$. The mA values were interpolated from experimentally obtained K per mA (not shown). All computations were repeated for the studied Sn and Cu filters and for 20 to 80 mm thick breasts with $f_g = 50\%$.

3 Results and Discussion

3.1 Optimal Weighting Factor w_t

Fig. 2 illustrates optimal w_t values as a function of the Sn-Cu filter pairs for 20 to 80 mm thick breasts with glandular tissue densities, f_g , between 0% and 50%. For a given filter pair, optimal w_t values are smaller for thinner breasts. This finding is important for the development of a clinical imaging system, since w_t has to be adjusted with breast thickness. For a given breast thickness, w_t varies as a function of filter combination. For thin breasts (20 and 40 mm breasts), the magnitude of w_t is almost independent of Sn thickness and varies only as a function of Cu thickness. For thicker breasts, w_t varies somewhat with Sn thickness, but varies greatly with Cu thickness. We found that these trends are related to the average energy differences between the detected Sn and Cu spectra (not shown); the optimal w_t is smaller when the energy difference between the detected Sn and Cu spectra is larger.

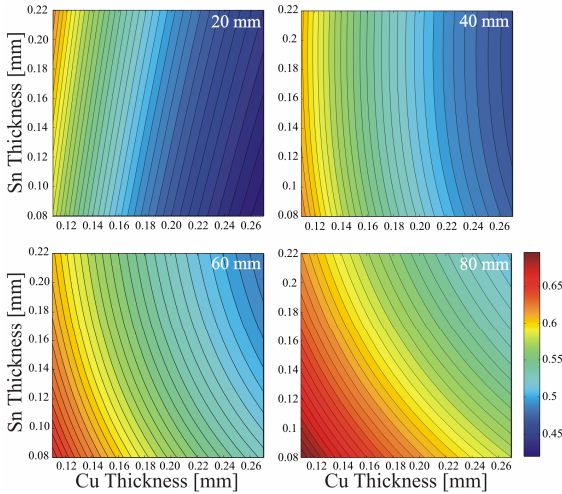


Fig. 2. Optimal w_t for the studied Sn-Cu filter pairs shown as a function of breast thickness (indicated in the right upper corner). For a given filter pair, w_t values are smaller for thinner breasts. Observe that for thin breasts w_t is almost independent of Sn thickness and varies only with Cu thickness. For thicker breasts w_t varies somewhat with Sn thickness, but varies greatly with Cu thickness.

3.2 Dose Allocation Optimization

Fig. 3 shows $SDNR/\sqrt{MGD_{Total}}$ as a function of MGD_{Cu}/MGD_{Total} and Cu thickness for 1 mg I/cm² embedded in a 40 mm thick flat breast background with $f_g = 50\%$. The Sn thickness is equal to 0.12 mm. Optimal w_t values were applied in the logarithmic subtraction. $SDNR/\sqrt{MGD_{Total}}$ has a broad maximum for intermediate

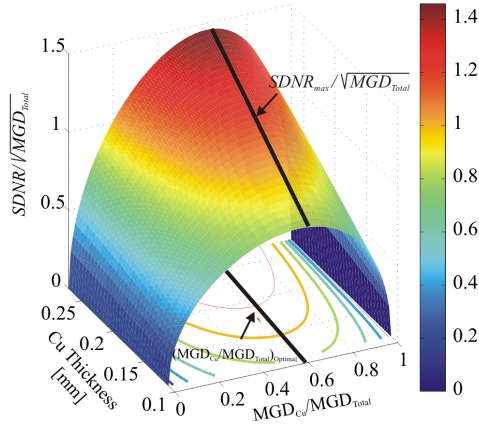


Fig. 3. $SDNR/\sqrt{MGD_{Total}}$ for 1 mg I/cm^2 embedded in a 40 mm thick breast ($f_g = 50\%$) as a function of MGD_{Cu}/MGD_{Total} and Cu filter thickness. The Sn filter thickness equals 0.12 mm. $SDNR_{max}/\sqrt{MGD_{Total}}$ ranges from 0.81 to 1.46.

MGD_{Cu}/MGD_{Total} values. This is desirable, since it is not that critical to operate a bit off the optimal MGD_{Cu}/MGD_{Total} .

Fig. 4 shows $SDNR_{max}/\sqrt{MGD_{Total}}$ as a function of the studied Sn-Cu filter pairs for 1 mg I/cm^2 in breasts with various thicknesses. Optimal w_t values are applied in the logarithmic subtraction. As expected $SDNR_{max}/\sqrt{MGD_{Total}}$ is larger for thicker breasts. For 20 mm thick breasts, $SDNR_{max}/\sqrt{MGD_{Total}}$ is almost independent of Sn thickness. With increasing breast thickness, the dependence of $SDNR_{max}/\sqrt{MGD_{Total}}$ on Sn filter thickness increases. $SDNR_{max}/\sqrt{MGD_{Total}}$ (Fig. 4) is inversely correlated with w_t (Fig. 2) because noise arising from the Sn image, $(\sigma_{Sn}^{DBT})^2$ is multiplied by w_t^2 .

Fig. 5 shows optimal MGD_{Cu}/MGD_{Total} values for all studied Sn-Cu filter pairs and for 20 to 80 mm thick breasts. MGD_{Cu} is greater than MGD_{Sn} for all breast thicknesses. Optimal MGD_{Cu}/MGD_{Total} values are smaller for thicker breasts. For a given breast thickness, MGD_{Cu}/MGD_{Total} varies as a function of filter combination. For 20 mm thick breasts the optimal MGD_{Cu}/MGD_{Total} is almost independent of Sn thickness. For 4 cm thick breasts, the optimal MGD_{Cu}/MGD_{Total} varies as a function of Sn and Cu thickness. For the 60 and 80 mm thick breasts, the optimal MGD_{Cu}/MGD_{Total} is almost independent of Cu thickness.

Since the Sn and Cu images are acquired simultaneously in our geometry, practical solutions require that the Sn and Cu images are acquired at the same mA. The Varian Rad-70 tube operated at 180 Hz and 49 kV is limited to a maximum tube current of 140 mA for the 10 second scan time. Because the Sn and Cu images are acquired simultaneously, MGD_{Cu}/MGD_{Total} is also fixed regardless of mA for a given Sn-Cu filter pair and breast and optimal MGD_{Cu}/MGD_{Total} is only obtained for a restricted set of Sn-Cu pairs. For the 1:1 and the 1:2 configurations, the Sn-Cu filter pair that

requires 140 mA and for which optimal MGD_{Cu}/MGD_{Total} values can be obtained was found to depend on breast thickness (not shown); this is impractical for a clinical system. Therefore feasible operating points, using the same Sn and Cu filter thickness for all breast thicknesses are proposed. For the 1:1 and 1:2 configurations, we chose to apply the filter combination that is optimal for the 80 mm thick breast because it has inherent the lowest $SDNR_{max}/\sqrt{MGD_{Total}}$. The feasible operation points were up to 11% off $SDNR_{max}/\sqrt{MGD_{Total}}$. For the 1:1 system configuration 0.120 mm Sn–0.135 mm Cu was chosen, for the 1:2 system configuration 0.090 mm Sn–0.170 mm Cu was chosen (Fig. 6). For the feasible operating points, the $SDNR/\sqrt{MGD_{Total}}$ values for the 1:2 system configuration are slightly higher than for the 1:1 system configuration for all breast thicknesses; the differences being larger for thin breasts than for thick breasts.

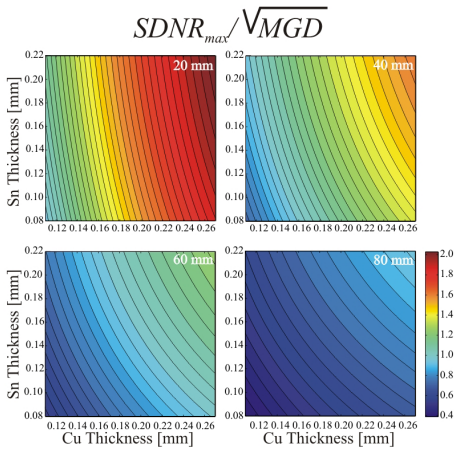


Fig. 4. $SDNR_{max}/\sqrt{MGD_{Total}}$ for a 1 mg/cm² areal iodine density as a function of breast thickness (indicated in the right upper corner)

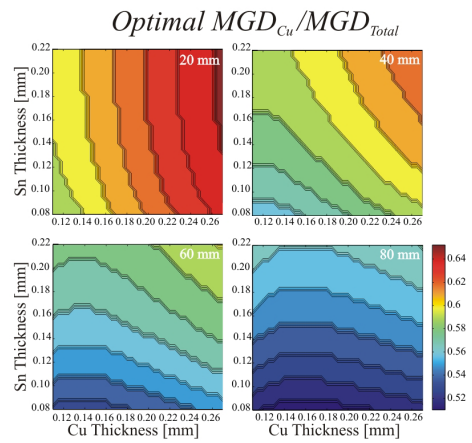


Fig. 5. Optimal MGD_{Cu}/MGD_{Total} as a function of the studied Sn–Cu filter pairs and for various breast thicknesses (indicated in the right upper corner)

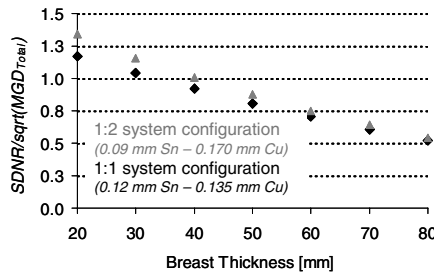


Fig. 6. $SDNR/\sqrt{MGD_{Total}}$ at feasible operating points for a 1 mg/cm² areal iodine density

4 Conclusion

Our DE CE-DBT subtraction technique acquires high- and low-energy images in a single scan by differentially filtering the 48 fan beams defined by a pre-patient collimator. In a clinical implementation our system design will greatly overcome motion artifacts. We believe that the proposed DE CE-DBT subtraction technique for the photon-counting XC Mammo-3T DBT system is capable of visualizing breast lesion vascularity. Our results encourage further investigation and optimization of DE CE-DBT as a diagnostic tool for breast cancer detection and differentiation.

Acknowledgment

We acknowledge the financial support of Philips Medical Systems/RSNA Research Seed Grant 2005, the Department of Defense for the Concept Award BC052803 and the National Cancer Institute Grant PO1-CA85484.

References

1. Schnall, M.D., Blume, J., Bluemke, et al.: Diagnostic architectural and dynamic features at breast MR imaging: multicenter study. *Radiology* 238(1), 42–53 (2006)
2. Chen, S.C., Carton, A.-K., Albert, M., Conant, E.F., et al.: Initial clinical experience with contrast-enhanced digital breast tomosynthesis. *Academic Radiology* 14, 229–238 (2007)
3. Carton, A.-K., Li, J., Albert, M., Chen, S., Maidment, A.D.: Quantification for contrast-enhanced digital breast tomosynthesis. In: Flynn, M.J., Hsieh, J. (eds.) *Proc. Medical Imaging 2006: Physics of Medical Imaging*, San Diego, vol. 6146, pp. 111–121 (2006)
4. Maidment, A.D.A., Albert, M., Thunberg, S., et al.: Evaluation of a Photon-Counting Breast Tomosynthesis Imaging System. In: Flynn, M.J. (ed.) *Proc. SPIE*, vol. 5745, pp. 572–582. SPIE, San Diego (2005)
5. Maidment, A.D.A., Ullberg, C., Lindman, K., et al.: Evaluation of a photon-counting breast tomosynthesis imaging system. In: Flynn, M.J., Hsieh, J. (eds.) *Proc. Medical Imaging 2006: Physics of Medical Imaging*, vol. 6142, SPIE, San Diego (2006)
6. Boone, J.M.: Normalized glandular dose (DgN) coefficients for arbitrary x-ray spectra in mammography: Computer-fit values of Monte Carlo derived data. *Medical Physics* 29(5), 869–875 (2002)
7. Carton, A.K., Lindman, K., Ullberg, C.K., Francke, T.: Dual-energy subtraction for contrast enhanced digital breast tomosynthesis. In: Hsieh, J., Flynn, M.J. (eds.) *Proc. Physics of Medical Imaging*, vol. 6510. SPIE, San Diego (2007)